Johann Radon Institute for
Computational and Applied Mathematics
Austrian Academy of Sciences (ÖAW)

Numerical approximation of water waves through a deterministic algorithm

D. Amann, K. Kalimeris

RICAM-Report 2017-37

Numerical approximation of water waves through a deterministic algorithm

D. Amann and K. Kalimeris

Radon Institute for Computational and Applied Mathematics, Austrian Academy of Sciences, Linz, Austria.

October 25, 2017

Abstract

Recently, a constructive algorithm based on asymptotic expansions was proposed for computing water waves of large amplitude, in the absence of stagnation points, in [4]. Here, we perform a numerical implementation of this algorithm, verifying the analytical results and, indeed, computing large amplitude waves. Furthermore, we introduce a modification of the existing analytical procedure, which allows the computation of waves with variable vorticity by a straightforward adaptation of the current algorithm. Profiles and other features of water waves are presented for constant and some cases of variable vorticity.

1 Introduction

The analysis of the water wave problem dates back to the studies of Newton and Stokes [10]; a detailed review on the origins of water wave theory is given in [3], where the main contributions until the great work of Stokes are presented. Since then, an abundance of work has been appeared. Not in few cases, a detailed insight on the studying of the problem and the properties of its solutions may be extracted through a combined application of analytical and numerical approaches.

In the present work, we study travelling periodic water waves in flows with underlying current of variable vorticity without stagnation points. In [2], starting from Euler's equations for two dimensional, periodic, travelling water waves with variable vorticity, and applying a partial-hodograph transformation, the nonlinear boundary value problem (1)-(3) was derived. A key role in the analysis of this problem is the occurrence of a bifurcation parameter which is indicative of the total energy of the wave; this parameter, denoted by Q, is called the hydraulic head of the flow.

Based on the above formulation, non-trivial solutions of (1)-(3) were obtained analytically in the form of asymptotic expansions in [1] and [4], for the case of constant vorticity. The latter work can be viewed as a non-trivial generalization of the former one. Furthermore, in [4] a constructive algorithm was proposed for the computation of higher order terms of these asymptotic expansions; the possibility of extending this algorithm for computing waves with variable vorticity was discussed therein.

The above-mentioned algorithm provided a precise way to compute the expansions to all orders, but it involved tedious, though straightforward calculations. Thus, the goal of the current work is two-fold:

- Firstly, we provide the numerical implementation of the above algorithm, i.e. we numerically compute higher–order terms of the above asymptotic expansions corresponding to waves of moderate and large amplitude; the details are in section 4. This includes numerical verification that the system (8) is satisfied and that the numerical solution of its individual step of the algorithm have the expected convergence.
- Secondly, we introduce a novel transformation in one of the main steps of the analytical procedure which was used in [4]. This allows the extension of the previous analytical solutions to problems with variable vorticity; the details are in section 2.2. Furthermore, this induces a slight modification on the numerical implementation in order to compute high-order expansions of flows with variable vorticity. Following this modification we display some features of such waves in section 4.2.

For the modelling of our problem we follow [2] where the considered problem, finding water waves with a free surface, is reformulated as a fixed–domain system by applying a Dubreil-Jacotin transformation. Then the problem is, for a given constant $p_0 < 0$ and vorticity function γ, to find $Q \in \mathbb{R}$ and a periodic, even function h satisfying

$$\mathcal{H}[h] := (1 + h_q^2)h_{pp} - 2h_p h_q h_{qp} + h_p^2 h_{qq} - \gamma(-p)h_p^3 = 0 \quad \text{in } R, \tag{1}$$

$$\mathcal{B}_0[h, Q] := 1 + h_q^2 + (2gh - Q)h_p^2 = 0 \quad \text{for } p = 0, \tag{2}$$

$$\mathcal{B}_1[h] := h = 0 \quad \text{for } p = p_0. \tag{3}$$

One family of solutions are so called laminar waves or parallel shear flows, those are solutions that only depend on p. With this assumption the system becomes significantly easier and can solved analytically for many vorticity functions. To emphasize the special character of laminar waves we denote such solutions as H, for example for linear vorticity

$$H(p; \lambda) = \frac{2(p - p_0)}{\sqrt{\lambda - 2\gamma p} + \sqrt{\lambda - 2\gamma p_0}}$$

where $\lambda > 0$ has to satisfy

$$Q = \lambda - \frac{4gp_0}{\sqrt{\lambda} + \sqrt{\lambda - 2\gamma p_0}}.$$

In general, there are no genuine waves in the neighbourhood of a laminar solution $(Q(\lambda), H(\lambda))$, see [2] for constant vorticity. For certain values of λ and Q, denoted as λ_* and Q^* respectively, a branch of non-laminar bifurcates from the curve of laminar flows. The values of λ_* and Q^* are determined by the dispersion relation, see [5].

We present an asymptotic expansion of a solution (Q, h) on the non-laminar branch around the solution $(Q^*, H(\lambda^*))$ for non-constant vorticity. Furthermore, the constructive algorithm for computing the expansion terms can be implemented only solving one-dimensional differential equations.

2 Asymptotic Expansion algorithm

In this section we aim to recap the constructive algorithm presented in [4], we refer to the original paper for more details and proofs. The main idea is to find an expansion of the pair (Q, h) around the bifurcation point (Q^*, H). Here and the remainder of this paper H without a specific λ is the laminar flow at the bifurcation point, that is $H(p) = H(p; \lambda_*)$.

We introduce approximations of the pair (Q, h) by the polynomials in $b \in \mathbb{R}$

$$Q \approx Q^{(2N)}(b) \qquad := Q^* + \sum_{k=1}^{N} Q_{2k} b^k \tag{4}$$

$$h(q, p; Q) \approx h^{(2N+1)}(q, p; b) := \sum_{k=0}^{2N+1} h_k(q, p) b^k \tag{5}$$

with coefficients $Q_{2k} \in \mathbb{R}$ and h_k defined as

$$h_{2k}(q, p) := \sum_{m=0}^{k} \cos(2mq) f_{2m}^{2k}(p), \tag{6}$$

$$h_{2k+1}(q, p) := \sum_{m=0}^{k} \cos((2m + 1)q) f_{2m+1}^{2k+1}(p) \tag{7}$$

where $f_m^k \in C^\infty([p_0, 0])$ for all m, k. The goal is to choose the constants Q_{2k} and functions f_m^k such that $(Q^{(2N)}, h^{(2N+1)})$ satisfies (1)–(3) up to $\mathcal{O}(b^{2N+2})$, that is

$$\begin{cases} \mathcal{H}[h^{(2N+1)}](q, p) & = \mathcal{O}(b^{2N+2}), \\ \mathcal{B}_0[h^{(2N+1)}, Q^{(2N)}](q) & = \mathcal{O}(b^{2N+2}), \\ \mathcal{B}_1[h^{(2N+1)}] & = 0. \end{cases} \tag{8}$$

We assume that the solution for $N = 0$, that is $Q^{(0)}$ and $h^{(1)}$ consisting of Q^*, h_0 and h_1 are known. These solutions are known analytically for irrotational waves with zero vorticity and a variety of rotational waves, see [5].

2.1 Zero vorticity

For ease of notation we discuss a irrotational case in this section in detail and explain the necessary modifications for more general vorticity in Section 2.2.

Assume $h^{(2N+1)}$ is known, the goal is to compute additional expansion terms h_{2N+2}, h_{2N+3} and Q_{2N+2}. The algorithm is split into two parts where first we compute h_{2N+2} and then the pair (h_{2N+3}, Q_{2N+2}).

Find h_{2N+2}**:** Let $h^{(2N+1)}$ be the known solution of our model problem (1)–(3) up to order b^{2N+2}, then set

$$\hat{h}^{(2N+2)} = h^{(2N+1)} + b^{2N+2} h_{2N+2}.$$

for a yet to be determined function h_{2N+2} of the form (6). Apply the operators $\mathcal{H}$ and $\mathcal{B}_0$ to $\hat{h}^{(2N+2)}$ gives us a polynomial in b. For example, the first term of $\mathcal{H}[\hat{h}^{(2N+2)}]$ looks like

$$\left[1+\left(\hat{h}_q^{(2N+2)}\right)^2\right]\hat{h}_{pp}^{(2N+2)} = \left[1+\left(\sum_{k=0}^{2N+2} b^k (h_k)_q\right)^2\right]\left(\sum_{\ell=0}^{2N+2} b^\ell (h_\ell)_{pp}\right).$$

We know that by definition all terms up to and including b^{2N+1} are equal to zero. Our goal is to find h_{2N+2} such that the coefficient belonging to b^{2N+2} vanishes as well. Furthermore, h_{2N+2} must satisfy the homogeneous Dirichlet boundary condition at $p = p_0$ and must be of the form (6). Setting the coefficients corresponding to b^{2N+2} of $\mathcal{H}[\hat{h}^{(2N+2)}]$ and $\mathcal{B}_0[Q^{(2N)}, \hat{h}^{(2N+2)}]$ to zero and collecting all known data on the right hand side gives us

$$\begin{aligned} (h_{2N+2})_{pp} + \frac{1}{\lambda^*}(h_{2N+2})_{qq} &= e^{(R)} \qquad && (q,p) \in R, \\ (h_{2N+2})_p - \frac{g}{\lambda_*^{3/2}} h_{2N+2} &= e^{(B)} && p = 0, \\ h_{2N+2} &= 0 && p = p_0. \end{aligned}$$

Note that we additionally scaled the boundary condition by $-\frac{1}{2\sqrt{\lambda_*}}$. Furthermore, from [4] we know that $e^{(R)}$ and $e^{(B)}$ can be written as

$$e^{(R)}(p) = \sum_{m=0}^{N+1} \cos(2mq) e_{2m}^{(R)}(p) \quad \text{and} \quad e^{(B)} = \sum_{m=0}^{N+1} \cos(2mq) e_{2m}^{(B)} \tag{9}$$

and the solution also has the form

$$h_{2N+2}(q,p) = \sum_{m=0}^{N+1} \cos(2mq) f_{2m}^{2N+2}(p).$$

The functions f_{2m}^{2N+2} for $m = 0, \ldots, N+1$ are found as solutions of the ordinary differential equation

$$(f_{2m}^{2N+2})_{pp} - \frac{(2m)^2}{\lambda^*} f_{2m}^{2N+2} = e_{2m}^{(R)}(p) \quad p \in (p_0, 0), \tag{10}$$

$$(f_{2m}^{2N+2})_p - \frac{g}{\lambda_*^{3/2}} f_{2m}^{2N+2} = e_{2m}^{(B)} \quad p = 0 \tag{11}$$

$$f_{2m}^{2N+2} = 0 \quad p = p_0 \tag{12}$$

Note that one could, as done in [4], already introduce Q_{2N+2} which would results in a different function h_{2N+2}. More precisely f_0^{2N+2} then has the form

$$f_0^{2N+2} = Q_{2N+2}\hat{f}_0(p) + \widetilde{f}_0^{2N+2}(p)$$

where $\hat{f}_0 = -\frac{1}{2}\frac{1}{gp_0+\lambda_*^{3/2}}(p-p_0)$ and $\widetilde{f}_0^{2N+2}$ does not depend on Q_{2N+2}. For every $Q_{2N+2} \in \mathbb{R}$ this provides a function f_0^{2N+2} that solves the system (which would also contain Q_{2N+2}) and we can for the moment choose $Q_{2N+2} = 0$.

The parameter Q_{2N+2} will be uniquely determined in the next step and we can update f_0^{2N+2} accordingly.

The so constructed pair $(Q^{(2N)}, \hat{h}^{(2N+2)})$ satisfies the systems (1)–(3) up to order $\mathcal{O}(b^{2N+3})$.

Find (Q_{2N+2}, h_{2N+3})**:** We set

$$
\begin{aligned}
h^{(2N+3)} &:= \hat{h}^{(2N+2)} + b^{2N+2} Q_{2N+2} \hat{f}_0 + b^{(2N+3)} h_{2N+3},\\
Q^{(2N+2)} &:= Q^{(2N)} + b^{(2N+2)} Q_{2N+2}.
\end{aligned}
$$

Here we have to include the contribution of $\hat{f}_0$ that we earlier omitted since otherwise the system we get would not be solvable as observed in [1]. Analogous to before we apply the operators $\mathcal{H}$, $\mathcal{B}_0$ and $\mathcal{B}_1$ to $(Q^{(2N+2)}, h^{(2N+3)})$, set the coefficient belonging to b^{2N+3} to zero and collect all known data in the right hand side $(s^{(R)}, s^{(B)})$. This results in the system

$$
(h_{2N+3})_{pp} + \frac{1}{\lambda^*}(h_{2N+3})_{qq} + Q_{2N+2} A(p)\cos(q) = s^{(R)}(q,p) \quad (q,p) \in R, \tag{13}
$$

$$
(h_{2N+3})_p - \frac{g}{\lambda_*^{3/2}} h_{2N+3} + Q_{2N+2} B \cos(q) = s^{(B)} \qquad p = 0 \tag{14}
$$

$$
h_{2k} = 0 \qquad p = p_0 \tag{15}
$$

The function A and constant B are the contributions related to Q_{2N+2} and thus $\hat{f}_0$. For the case of zero vorticity they are given by

$$
\begin{aligned}
A(p) &= \frac{1}{\sqrt{\lambda_*}} \frac{1}{g p_0 + \lambda_*^{3/2}} \sinh\left(\frac{p - p_0}{\sqrt{\lambda_*}}\right),\\
B &= \frac{3}{2} \frac{1}{g p_0 + \lambda_*^{3/2}} \cosh \frac{p_0}{\sqrt{\lambda_*}}.
\end{aligned}
$$

Similar to before the right hand side has the structure

$$
s^{(R)}(p) = \sum_{m=0}^{N+1} \cos((2m+1)q) s_{2m+1}^{(R)}(p) \quad \text{and} \quad s^{(B)} = \sum_{m=0}^{N+1} \cos((2m+1)q) s_{2m+1}^{(B)}
$$

and so has the solution

$$
h_{2N+3}(q,p) = \sum_{m=0}^{N+1} \cos((2m+1)q) f_{2m+1}^{2N+3}(p).
$$

Special care has to be taken of $m = 0$, that is the system that includes Q_{2N+2} with $A(p)$ and B. The system reads

$$
\begin{aligned}
(f_1^{2N+3})_{pp} - \frac{1}{\lambda^*} f_1^{2N+3} + Q_{2N+2} A(p) &= s_1^{(R)}(p) \quad && p \in (p_0, 0),\\
(f_1^{2N+3})_p - \frac{g}{\lambda_*^{3/2}} f_1^{2N+3} + Q_{2N+2} B &= s_1^{(B)} && p = 0\\
f_1^{2N+3} &= 0 && p = p_0.
\end{aligned}
$$

This system is not solvable for all values of Q_{2N+2}. To find an admissible Q_{2N+2} we consider a function that solve the first and third equation of this system. Such a function has the form

$$
f_1^{2N+3}(p) = Q_{2N+2}\alpha(p) + \beta(p) + \mathcal{C} \sinh \frac{p - p_0}{\sqrt{\lambda_*}}
$$

for an arbitrary constant $\mathcal{C}$. The function $\alpha(p)$ depends on A and $\beta(p)$ depends on the right hand side $s_1^{(R)}$. Inserting this into the Robin boundary condition gives

$$\left(\alpha'(0) - \frac{g}{\lambda_*^{3/2}}\alpha(0)\right) Q_{2N+2} + \beta'(0) - \frac{g}{\lambda_*^{3/2}}\beta(0) + BQ_{2N+2} = s_1^{(B)}.$$

Note that the contribution of the term $\mathcal{C}\sinh\frac{p-p_0}{\sqrt{\lambda_*}}$ is zero. From this equation we see that Q_{2N+2} has to satisfy an equation of the form

$$\mathcal{C}_1 Q_{2N+2} = \mathcal{C}_2.$$

The constant $\mathcal{C}_1$ only depends on A and B and thus on the vorticity, but not on N. For the irrotational case it is given by

$$\mathcal{C}_1 = -\frac{1}{2\lambda_*^{3/2}} \frac{\sqrt{\lambda_*}(2g + p_0\sqrt{\lambda_*})\sinh(\frac{p_0}{\sqrt{\lambda_*}}) + gp_0\cosh(\frac{p_0}{\sqrt{\lambda_*}})}{gp_0 + \lambda_*^{3/2}}.$$

Note that since $\mathcal{C}$ can be chosen arbitrarily, so f_1^{2N+3} is not uniquely determined. For our numerical implementation we need to introduce and suitable constraint, see Section 3.3. Other strategies for choosing $\mathcal{C}$ lead to other solutions but all of theme satisfy (1)–(3) up to the desired order.

With this found h_{2N+3} and Q_{2N+2} and hence

$$\begin{aligned} Q^{(2N+2)} &= Q^{(2N+2)} + b^{N+1}Q_{2N+2}, \\ h^{(2N+3)} &= h^{(2N+1)} + b^{2N+2}\left(h_{2N+2} + Q_{2N+2}\hat{f}_0\right) + b^{2N+3}h_{2N+3}. \end{aligned}$$

2.2 Non zero vorticity

In this section we discuss how this procedure can be applied if the vorticity is not equal to zero but a function $\gamma(-p)$. Instead of working with the system as is, we will transform it to an equivalent system of the form (10)–(12) to unify our numerical considerations. A similar transformation was used in [1, 4], the transformation presented here has the advantage to work for general vorticities $\gamma \in C^1$.

Let $h^{(2N+1)}$ be known, then as in Section 2, we apply $\mathcal{H}$ and $\mathcal{B}_0$ to $h^{(2N+1)} + b^{2N+2}h_{2N+2}$ for a function h_{2N+2} of the form (6). Setting the coefficient belonging to b^{2N+2} to zero gives us the system

$$\begin{aligned} (h_{2N+2})_{pp} - 3\gamma(H')^2(h_{2N+2})_p + (H')^2(h_{2N+2})_{qq} &= e^{(R)} && (q,p) \in R, \\ (h_{2N+2})_p - \frac{g}{\lambda_*^{3/2}}(h_{2N+2}) &= e^{(B)} && p = 0, \\ h_{2N+2} &= 0 && p = p_0. \end{aligned}$$

Here the function H is the solution of the laminar problem and first term of the expansion $H = h_0$ which is a q-independent function. Exploiting the structure of the right hand side as well as h_{2N+2}, see (6), and separation of variables gives us

$$(f_{2m}^{2N+2})'' - 3\gamma(H')^2(f_{2m}^{2N+2})' - (2mH')^2 f_{2m}^{2N+2} = e_{2m}^{(R)}(p) \quad p \in (p_0, 0), \tag{16}$$

$$(f_{2m}^{2N+2})' - \frac{g}{\lambda_*^{3/2}} f_{2m}^{2N+2} = e_{2m}^{(B)} \quad p = 0, \tag{17}$$

$$f_{2m}^{2N+2} = 0 \quad p = p_0. \tag{18}$$

If there exists a shear flow $H = h_0$ that solves the laminar problem, then it follows form [2] that $H'(p) > 0$ for all $p \in (p_0, 0)$ which allows us the change of variables from p to $H(p)$. With this transformation we define

$$f_{2m}^{2N+2}(p) = \tilde{f}_{2m}^{2N+2}(H(p))H'(p),$$

which leads to a system that is equivalent to (16)–(18)

$$\begin{aligned}
\frac{d^2}{dH^2}\tilde{f}_{2m}^{2N+2}(H) + \left[\frac{d}{dp}\gamma(p(H)) - (2m)^2\right]\tilde{f}_{2m}^{2N+2}(H) &= \tilde{e}_{2m}^{(R)}(H) \quad && H \in (0, H(0)),\\
\frac{d}{dH}\tilde{f}_{2m}^{2N+2}(H) + \frac{\gamma(0)\sqrt{\lambda_*} - g}{\lambda_*}\tilde{f}_{2m}^{2N+2}(H) &= \tilde{e}_{2m}^{(B)} && H = H(0),\\
\tilde{f}_{2m}^{2N+2}(H) &= 0 && H = 0.
\end{aligned}$$

The right hand side is given by

$$\tilde{e}_{2m}^{(R)}(H) = \frac{e_{2m}^{(R)}(p(H))}{(H')^3} \qquad \text{and} \qquad \tilde{e}_{2m}^{(B)} = \lambda_* e_{2m}^{(B)}.$$

In case of linear vorticity the derivative $\frac{d}{dp}\gamma$ is constant and so the system is of the same form as in the zero vorticity case. For more general functions $\gamma(-p)$, like quadratic vorticity, we need the inverse of the transform $p(H)$ which is not available analytically but can be done numerically for computation purposes. This allows us to restrict our numerical considerations to system of the form (10)–(12).

A second notable difference to the irrotational case considered in Section 2.1 is that $\hat{f}_0$, the part of f_0^{2N+2} that depends on Q_{2N+2}, is in general not known. Instead, we use the definition of $\hat{f}_0$ as the solution of

$$\begin{aligned}
\hat{f}_0'' - 3\gamma(H')^2\hat{f}_0' &= 0 \qquad && p \in (p_0, 0),\\
\hat{f}_0' - \frac{g}{\lambda_*^{3/2}}\hat{f}_0 &= -\frac{1}{2\lambda_*^{3/2}} && p = 0,\\
\hat{f}_0 &= 0 && p = p_0.
\end{aligned}$$

Once we computed $\hat{f}_0$ we can apply the operators $\mathcal{H}$ and $\mathcal{B}_0$ which gives us $A(p)$ and B respectively and allows us to compute Q_{2N+2}.

3 Numerical Approximation

Given $(Q^{(2N)}, h^{(2N+1)})$, our aim is compute Q_{2N+2} as well as h_{2N+3} and h_{2N+2} while preserve their structure (6) and (7) respectively. Thus we need to find approximations of

$$\begin{aligned}
&f_{2m}^{2N+2}(p) \qquad && m = 0, \dots, N+1,\\
&f_{2m+1}^{2N+3}(p) && m = 0, \dots, N+1.
\end{aligned}$$

To find these functions, we need to solve systems whose right hand side include $f_{2m}^{2k}(p)$ and $f_{2m+1}^{2k+1}(p)$ for $k \leq N$ as well as their first and second derivatives, which we must assume are also just approximations. Since the approximations can at best be as good as the input data, i.e. the right hand side, we need to ensure that f and its derivatives up to second order have the same order of convergence.

To summarize, our goal is to find approximations of Q_{2N+2} and

$$\begin{aligned} &f_{2m}^{2N+2}, (f_{2m}^{2N+2})', (f_{2m}^{2N+2})'' \qquad m = 0, \dots, N+1, \\ &f_{2m+1}^{2N+3}, (f_{2m+1}^{2N+3})', (f_{2m+1}^{2N+3})'' \qquad m = 0, \dots, N+1. \end{aligned}$$

where all orders of convergence should match. For this we follow the algorithm outlined in Section 2 and substitute approximations where necessary. Section 3.1 explains how the right hand side of (10)–(12) and (13)-(15) is computed. How to solve the resulting systems is considered in Sections 3.2 and 3.3 for uniquely solvable and singular systems respectively.

3.1 Construction of right hand side

We only consider in detail part of a specific case to illustrate the procedure described in detail in [4], the remaining part of the right hand side can be computed accordingly. Let $h^{(2N+1)}$ be known, then we are interested in the b^{2N+2}-coefficient of $\mathcal{H}[h^{(2N+1)}]$, which is the first non-zero coefficient. Here we consider the third term of $\mathcal{H}[h^{(2N+1)}]$, that is

$$h_q^{(2N+1)} h_q^{(2N+1)} h_{pp}^{(2N+1)} = \sum_{k_1=0}^{2N+1} b^{k_1} (h_{k_1})_q \sum_{k_2=0}^{2N+1} b^{k_2} (h_{k_2})_q \sum_{k_3=0}^{2N+1} b^{k_3} (h_{k_3})_{pp}.$$

Since we are only interested in the terms belonging to b^{2N+2}, let K be the set of all tuples (k_1, k_2, k_3) such that $\sum_{i=1}^{3} k_i = 2N+2$ and $0 \leq k_i \leq 2N+1$ for $i = 1, 2, 3$. We must therefore compute

$$\sum_{(k_1,k_2,k_3)\in K} (h_{k_1})_q (h_{k_2})_q (h_{k_3})_{pp}. \tag{19}$$

To facilitate the distinction between odd and even cases of k_i we introduce the auxiliary functions

$$N(k_i) = \begin{cases} \frac{k_i-1}{2} & k_i \text{ odd} \\ \frac{k_i}{2} & k_i \text{ even} \end{cases},$$

$$n_{k_i}(m) = \begin{cases} 2m+1 & k_i \text{ odd} \\ 2m & k_i \text{ even} \end{cases}.$$

Now we consider one term of (19) and replace h_k by its definition

$$\begin{aligned}
(h_{k_1})_q(h_{k_2})_q(h_{k_3})_{pp} &= \sum_{m_1=0}^{N(k_1)} \cos'(n_{k_1}(m_1)q) f^{k_1}_{n_{k_1}(m_1)} \sum_{m_2=0}^{N(k_2)} \cos'(n_{k_2}(m_2)q) f^{k_2}_{n_{k_2}(m_2)} \\
&\quad \sum_{m_3=0}^{N(k_3)} \cos(n_{k_3}(m_3)q) \left[f^{k_3}_{n_{k_3}(m_3)} \right]'' \\
&= \sum_{m_1}^{N(k_1)} \sum_{m_2}^{N(k_2)} \sum_{m_3}^{N(k_3)} \Big\{ \sin(n_{k_1}(m_1)q) \sin(n_{k_2}(m_2)q) \cos(n_{k_3}(m_3)q) \\
&\qquad f^{k_1,k_2,k_3}_{m_1,m_2,m_3} \Big\} \\
&= \sum_{\ell=0}^{N+1} \cos(2\ell q) e^{(k_1,k_2,k_3)}_{2\ell}(p).
\end{aligned}$$

In the last step we exploited the known structure of the right hand side (9) which means that for all valid values k_i and m_i it holds

$$\sin(n_{k_1}(m_1)q) \sin(n_{k_2}(m_2)q) \cos(n_{k_3}(m_3)q) = \sum_{\ell=0}^{N+1} \cos(2\ell q) c^{k_1,k_2,k_3}_{m_1,m_2,m_3,2\ell}.$$

Now we collect all summands with the same value ℓ to get the desired result. Keeping track of the values k_i and $n_{k_i}(m_i)$ allows us to implement these computations exactly, no approximation in q-direction is necessary.

Finally, (19) can be written as

$$\begin{aligned}
\sum_{(k_1,k_2,k_3)\in K} (h_{k_1})_q(h_{k_2})_q(h_{k_3})_{pp} &= \sum_{(k_1,k_2,k_3)\in K} \sum_{\ell=0}^{N+1} \cos(2\ell q) e^{(k_1,k_2,k_3)}_{2\ell}(p) \\
&= \sum_{\ell=0}^{N+1} \cos(2\ell q) e_{2\ell}(p)
\end{aligned}$$

Doing the same for the other two terms of $\mathcal{H}[h^{(2N+1)}]$ and adding all three terms up yields the right hand side of (10) in the required series representation. The right hand side of the boundary condition (11) can be computed in the same manner but instead of functions $f^{k_i}_{n_{k_i}}$ we have to consider function evaluations at $p = 0$.

3.2 Solving the system

In this section we analyse systems of the form (10)–(12) where we applied separation of variables so that we only have to consider one–dimensional systems. These systems will be solved using a finite element approach, for more details on this see [9]. This section aims to be self–contained to avoid confusion due to notation. Where possible, we avoided to reuse symbols but in some cases, such as the mesh width h, that is not feasible.

Let $\Omega = (a, b)$, $e^{(\Omega)} \in C^\infty(\Omega)$, $e^{(b)} \in \mathbb{R}$, $\alpha \geq 0$. Find $u \in H^1_0(\Omega, a)$ as the weak solution of

$$u'' - \alpha u = e^{(\Omega)} \qquad x \in \Omega, \tag{20}$$

$$u' - \beta u = e^{(b)} \qquad x = b, \tag{21}$$

$$u = 0 \qquad x = a. \tag{22}$$

In this section we assume that the system is uniquely solvable. The case of a singular system, see $f_1^{(2k+1)}$, is considered in Section 3.3. The Dirichlet boundary conditions motivates the trial and test space

$$H_0^1(\Omega, a) := \{v \in H^1(\Omega) : v(a) = 0\}.$$

The point wise evaluation of $v \in H^1(\Omega)$ is well defined since in the considered one dimensional case it holds $H^1(\Omega) \subset C(\Omega)$. The associated variational formulation is to find $u \in H_0^1(\Omega, a)$ that satisfies

$$a(u, v) - c(u, v) = -\langle e^{(\Omega)}, v\rangle_{L_2(\Omega)} + e^{(b)} v(b) \qquad \forall v \in H_0^1(\Omega, a) \tag{23}$$

with

$$\begin{aligned} a(u, v) &:= \int_\Omega u'(x)v'(x)dx + \alpha \int_\Omega u(x)v(x)dx, \\ c(u, v) &:= \beta u(b)v(b). \end{aligned}$$

The symmetric and bounded bilinear form $a(\cdot, \cdot)$ is $H_0^1(\Omega, a)$–elliptic by standard arguments and the non negativity of α. Before we discuss $c(\cdot, \cdot)$ let $v \in H_0^1(\Omega, a)$ and $x \in \Omega$ and consider

$$\begin{aligned} v(x) &= \int_a^x v'(s)ds \\ &\leq \int_a^b |v'(s)|ds \\ &\leq \left(\int_a^b |v'(s)|^2 ds\right)^{1/2} |\Omega|^{1/2} \\ &= c|v|_{H^1(\Omega)}. \end{aligned}$$

Furthermore it follows

$$\|v\|_\infty = \sup_{x\in\Omega} |v(x)| \leq c \|v\|_{H^1(\Omega)}. \tag{24}$$

We want to show that the operator $C : H^1(\Omega) \to H^{-1}(\Omega)$, induced by the symmetric and bounded bilinear form

$$c(u, v) = \langle Cu, v\rangle_{H^1(\Omega)} = \beta u(b)v(b),$$

is compact. An operator $C : X \to X'$ is said to be compact if for any bounded sequence $\{u_n\}_{n\in\mathbb{N}} \subset X$, the sequence $\{Cu_n\}_{n\in\mathbb{N}} \subset X'$ contains a Cauchy subsequence. The boundedness follows directly from applying (24) to the definition of the norm

$$\|Cu\|_{H^{-1}(\Omega)} = \sup_{v\in H^1, \|v\|=1} |\langle Cu, v\rangle_{H^1(\Omega)}| = \sup_{v\in H^1, \|v\|=1} |\beta u(b)v(b)|.$$

Lemma 1. *The operator C is compact.*

Proof. Let $\{v_n\}_n \subset H^1(\Omega)$ be a bounded sequence such that $\|v_n\|_{H^1} \leq M \ \forall n$, then $v_n(b) \leq \|v_n\|_\infty \leq cM$. So $\{v_n(b)\}_n \subset \mathbb{R}$ is a bounded sequence and has, according to Bolzano Weierstra, a Cauchy subsequence $\{v_{n_\ell}(b)\}_\ell$. For every $\varepsilon > 0$ there exists $N_\varepsilon \in \mathbb{N}$ such that

$$|v_{n_k}(b) - v_{n_\ell}(b)| \leq \varepsilon \qquad \forall k, \ell \geq N_\varepsilon.$$

Let $k, \ell \geq N_\varepsilon$ and consider

$$\begin{aligned} \|Cv_{n_k} - Cv_{n_\ell}\|_{H^{-1}} &= \|C_2(v_{n_k} - v_{n_\ell})\|_{H^{-1}} \\ &\leq c|\beta||v_{n_k}(b) - v_{n_\ell}(b)| \\ &\leq c|\beta|\varepsilon \end{aligned}$$

Thus $\{Cv_{n_\ell}\}_\ell$ is a Cauchy sequence in H^{-1} which proves that C compact is. □

To summarise we have shown $H_0^1(\Omega, a)$–ellipticity of $a(\cdot, \cdot)$ and compactness of $c(\cdot, \cdot)$. Together with the assumed injectivity of (20)–(22) we can employ Fredholms alternative that shows unique solvability of the variational formulation (23).

We discretize the test and trial space $H_0^1(\Omega, a)$ by the space of piece wise linear, globally continuous functions $S_h^1(\Omega_h)$ with an equidistant grid Ω_h with mesh width h. A standard finite element approximation $u_h \in S_h^1(\Omega_h)$ of u leads to a uniquely solvable discrete system and error estimates [8, 9]

$$\|u - u_h\|_{L_2(\Omega)} \leq ch^2 \|u''\|_{L_2(\Omega)}, \qquad \|u - u_h\|_{L^\infty(\Omega)} \leq ch^2 \ln(h) \|u''\|_{L_2(\Omega)}.$$

As was established in Section 3.1 we need to ensure convergence rates not only of u but also u' and u''. To this end we introduce the piece wise linear, globally continuous approximations t_h of u' and s_h of u''. Define s_h as a reformulation of (20)

$$s_h = e^{(\Omega)} + \alpha u_h. \qquad \in \Omega,$$

then it follows immediately that s_h converges to s in the $L_2(\Omega)$-norm quadratically. The approximation t_h of u' is found by integrating

$$\begin{aligned} t_h' &= s_h & x &\in \Omega, \\ t_h &= e^{(b)} + \beta u_h & x &= b. \end{aligned}$$

Using Simpson quadrature rule and convergence properties of u_h we find that t_h admits the same convergence rates as u_h, that is quadratic in $L_2(\Omega)$ and quadratic up to a logarithmic factor in $L_\infty(\Omega)$.

3.3 Solving the singular system

Consider the same problem as in the previous Section, but without assuming injectivity. Let $\Omega = [a, b]$, $e^{(\Omega)} \in C^\infty$, $e^{(b)} \in \mathbb{R}$, $\alpha \geq 0$ and $b \in \mathbb{R}$. Find $u \in H_0^1(\Omega, a)$ as the weak solution of

$$\begin{aligned} u'' - \alpha u &= e^{(\Omega)} & x &\in \Omega, \\ u' - \beta u &= e^{(b)} & x &= b, \\ u &= 0 & x &= a. \end{aligned}$$

Then the homogeneous variational formulation

$$a(u,v) - c(u,v) = 0 \qquad \forall v \in H_0^1(\Omega, a)$$

has non trivial solutions. In fact, these homogeneous solutions are known, for the zero vorticity case they are of the form $u_0 := \kappa \sinh\left(\frac{p-p_0}{\sqrt{\lambda_*}}\right)$ with $\kappa \in \mathbb{R}$. In particular it holds for all considered vorticities $\int_\Omega u_0 \neq 0$ for $\kappa \neq 0$, so a suitable constraint for the solution u is

$$\int_\Omega u dx = \langle u, 1\rangle_{L_2(\Omega)} = 0.$$

We incorporate this constraint into our variational formulation as a saddle point formulation to find $(u,\eta) \in H_0^1(\Omega, a) \times \mathbb{R}$

$$\begin{aligned} a(u,v) - c(u,v) + \eta\langle v, 1\rangle_{L_2(\Omega)} &= F(v) \\ \langle u, 1\rangle_{L_2(\Omega)} &= 0 \end{aligned}$$

Using u_0 as a test function we get $\eta = 0$ so it is therefore equivalent to find

$$\begin{aligned} a(u,v) - c(u,v) + \eta\langle v, 1\rangle_{L_2(\Omega)} &= F(v) \\ \langle u, 1\rangle_{L_2(\Omega)} - \frac{\eta}{\mu} &= 0 \end{aligned}$$

with a scaling parameter $\mu \in \mathbb{R} \setminus \{0\}$ we can choose freely. In all our numerical experiments we have chosen the value $\mu = 1$. This variational formulation is further equivalent to

$$a(u,v) - c(u,v) + \mu\langle u, 1\rangle_{L_2(\Omega)}\langle v, 1\rangle_{L_2(\Omega)} = F(v)$$

This motivates the definition of a new bilinear form

$$\widetilde{a}(u,v) := a(u,v) + \mu\langle u, 1\rangle_{L_2(\Omega)}\langle v, 1\rangle_{L_2(\Omega)}$$

that is still symmetric, $H_0^1(\Omega, a)$–elliptic and bounded. So the system

$$\widetilde{a}(u,v) - c(u,v) = F(v) \qquad \forall v \in H_0^1(\Omega, a)$$

is still coercive, but now also injective. The remaining analysis of the variational formulation follows as in Section 3.2.

4 Numerical results

For our numerical experiments we choose the parameters in the considered systems (1)–(3) as $p_0 = -2$ and $g = 9.8$ in accordance with the numerical tests in [4, 1]. To distinguish between analytical and approximate functions and values we mark all approximations with a sub-index h.

The computation domain is either the interval $\Omega = (p_0, 0)$ which is divided into equidistant elements or its transformation as described in Section 2.2. On this mesh Ω_h we define the space of piece wise linear, globally continuous functions $S_h^1(\Omega)$. All approximate functions, i.e. $f_{m,h}^k \approx f_m^k$, $s_{m,h}^k \approx (f_m^k)'$ and $t_{m,h}^k \approx (f_m^k)''$ are defined as elements of $S_h^1(\Omega)$. If two or more functions are multiplied, then their product is projected back into the space $S_h^1(\Omega)$. The assembly and solution of the finite element system and everything related to it, like the previously mentioned projections, are implemented using the dolfin library [6, 7], part of the FEniCS project.

Note that this algorithm does not include any approximations of the q–dependent trigonometric functions. We simply keep track of the coefficient inside and if its a sin or a cos function. The only computations necessary are integrals of the form

$$\int_{-\pi}^{\pi} \cos(a_0 q) \sin(a_1 q) \sin(a_2 q) \sin(a_3 q) dq$$

which can be cone exactly.

4.1 Irrotational waves

First we test the convergence of our approximate solution as we increase the number of elements used to discretize Ω. Figure 1 shows the relative error of the $f_{m,h}^k$ in the $L_2(\Omega)$-norm as well as the relative error of the constants $Q_{k,h}$. The reference values used are analytical forms given in [4] up to h_5 and Q_4, and approximate solutions computed for 8192 grid points for terms of higher order. We observe the expected quadratic convergence for all $f_{m,h}^k$ and $Q_{k,h}$.

A second consideration is the residual of the operators $\mathcal{H}$ and $\mathcal{B}_0$ as we increase the number of expansions terms. Table 1 shows the results when we fix $Q = 22.05$ and use 512 elements. Fixing Q means that for every pair $(Q_h^{(2N)}, h_h^{(2N+1)})$ we have to determine b such that $Q_h^{(2N)}(b) = 22.05$, for the shown data it holds $b \in [0.1309, 0.1409]$. As one would expect, the residuals decrease as more expansion terms are added. This behaviour is not guaranteed and depends on the considered Q, values closer to Q^* lead to smaller values of b and a steeper decline, see Table 2, while for too large values of Q the residuals might diverge.

The third column in Table 1 is the relative low order error. Applying the operator $\mathcal{H}$ to the approximate solution $h_h^{(2N+1)}$ yields a polynomial in b, namely $\mathcal{H}[h_h^{(2N+1)}] = \sum_{k=0}^{6N+3} b^k r_k$. For an analytical solution it holds $r_k = 0$ for $k \leq 2N+1$ and r_{2N+2} is the first non-zero term. This motivates the definition of the error

$$E_{\text{LO}}\left(h_h^{(2N+1)}\right) = \max_{k=0,\ldots,2N+1} \frac{\|r_k\|_{L_2}}{\|r_{2N+2}\|_{L_2}} \tag{25}$$

where r_k is defined as above. Note that the contribution of this error to the total error is very small since it is additionally multiplied with b^k. We observe in Table 1 that the terms up to order $2N+1$ are almost zero as we would expect.

After confirming our algorithm and implementation, we display some characteristics of the irrotational wave. Figure 2 shows the bifurcation diagrams for the wave height and depth as we take more expansion terms into account. Figure 3a shows the streamlines of the irrotational wave at $Q = 22.05$, that is the same wave as studied in Table 1 with wave height ≈ 0.216.

For Figure 5 we fixed the residual at 10^{-4} and displayed the waves we observe for different values of N. The residual was chosen rather large so that for the first order approximation a distinction from the shear flow is still visible. We see

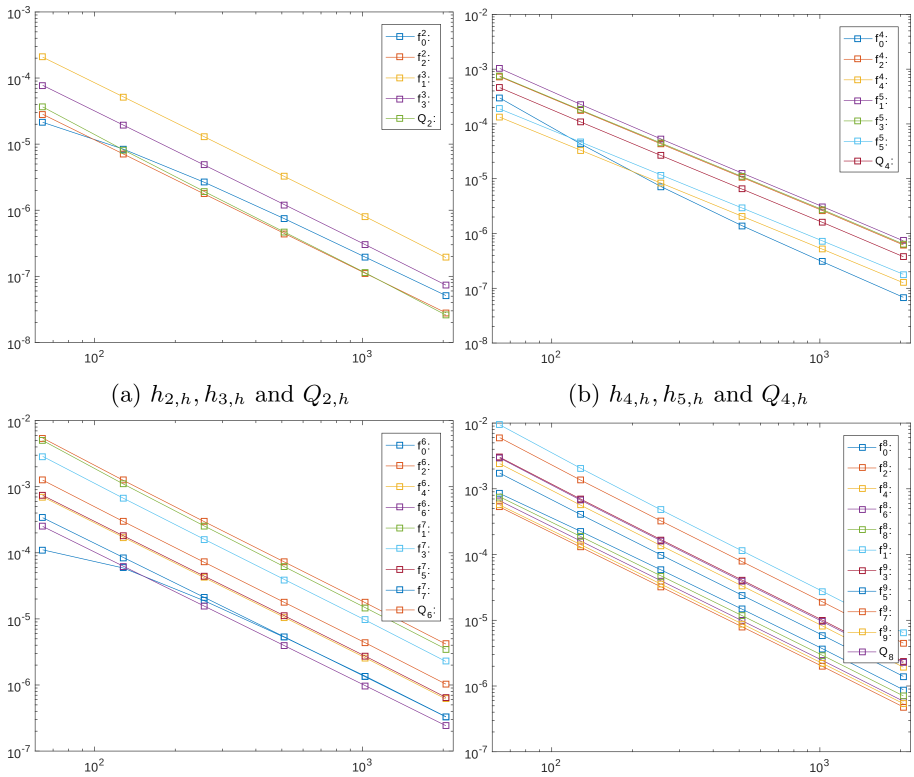

(a) $h_{2,h}, h_{3,h}$ and $Q_{2,h}$ (b) $h_{4,h}, h_{5,h}$ and $Q_{4,h}$

(c) $h_{6,h}, h_{8,h}$ and $Q_{6,h}$ (d) $h_{8,h}, h_{9,h}$ and $Q_{8,h}$

Figure 1: $||f_m^k - f_{m,h}^k||_{L_2}$ and $|Q_k - Q_{k,h}|$ vs. degrees of freedom, $\gamma = 0$.

	$\|\|\mathcal{H}[h_h^{(2N+1)}]\|\|_{L_2}$	$\|B_0[h_h^{(2N+1)}, Q_h^{(2N)}]\|$	$E_{\text{LO}}(h_h^{(2N+1)})$
$Q_h^{(2)}, h_h^{(3)}$	8.21E-03	1.04E-02	1.03E-16
$Q_h^{(4)}, h_h^{(5)}$	2.21E-03	2.57E-03	1.64E-16
$Q_h^{(6)}, h_h^{(7)}$	6.41E-04	7.46E-04	2.48E-16
$Q_h^{(8)}, h_h^{(9)}$	3.27E-04	3.16E-04	1.78E-16
$Q_h^{(10)}, h_h^{(11)}$	1.06E-04	9.84E-05	2.37E-16
$Q_h^{(12)}, h_h^{(13)}$	3.34E-05	3.43E-05	2.07E-16
$Q_h^{(14)}, h_h^{(15)}$	1.41E-05	1.35E-05	5.12E-16

Table 1: Residual of the differential and boundary operator for $Q = 22.05$ and the relative low order error E_{LO} (25), $\gamma = 0$

that higher order approximations allow for far larger waves while maintaining a similar residual.

4.2 Rotational waves

Here we present similar result as in Section 4.1 but for non-zero vorticity. Figure 6 shows the relative errors for $\gamma = 1$ as we decrease the mesh width. As in the

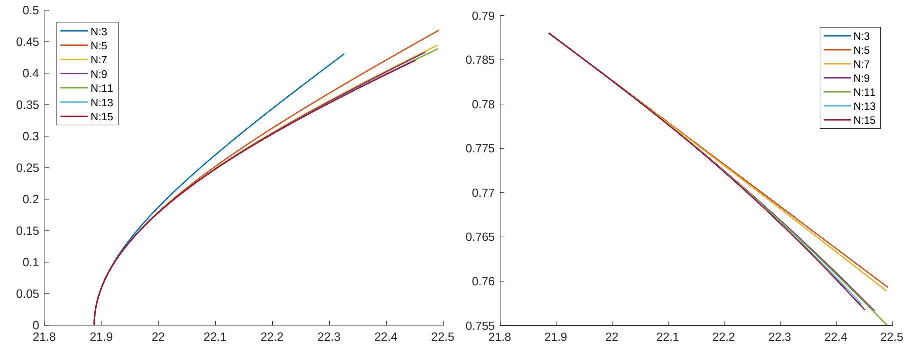

(a) Q, wave height (b) Q, depth

Figure 2: Bifurcation diagrams for expansions $(Q_h^{(2N)}, h_h^{(2N+1)})$ for $N = 1, \ldots, 7$, $\gamma = 0$.

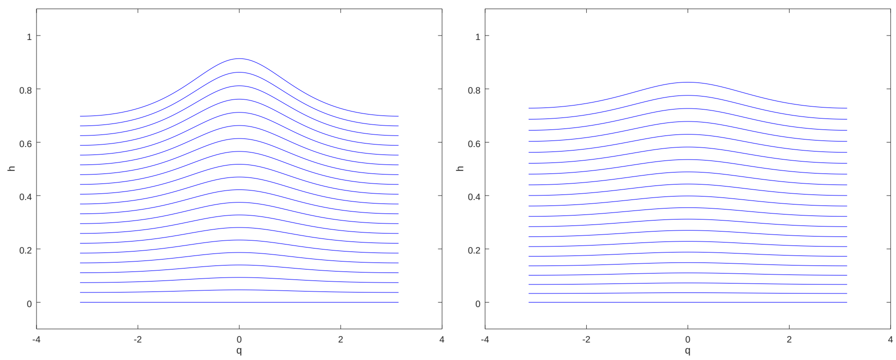

(a) $Q = 22.05$, $\gamma = 0$ (b) $Q = 21.69$, $\gamma(-p) = p$

Figure 3: Streamlines of $h_h^{(13)}$ for the waves considered in Tables 1 and 2.

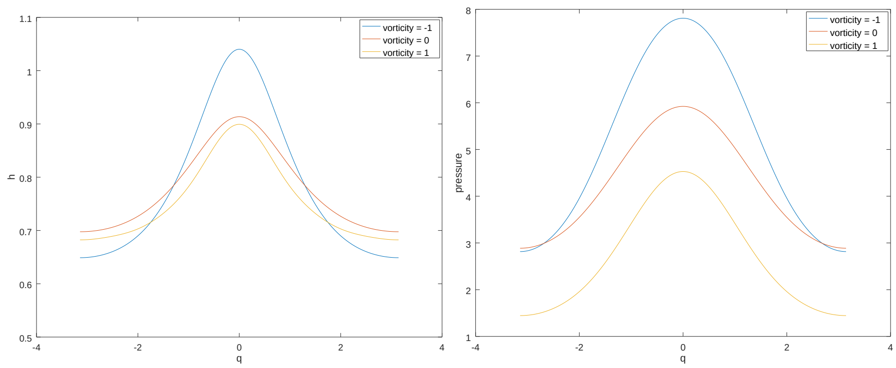

(a) Waveprofile (b) Pressure at $p = p_0$

Figure 4: Comparison of three waves with constant but different γ. Waves are chosen such that the residual are similar, reference was $\gamma = 0$ with $Q = 22.05$.

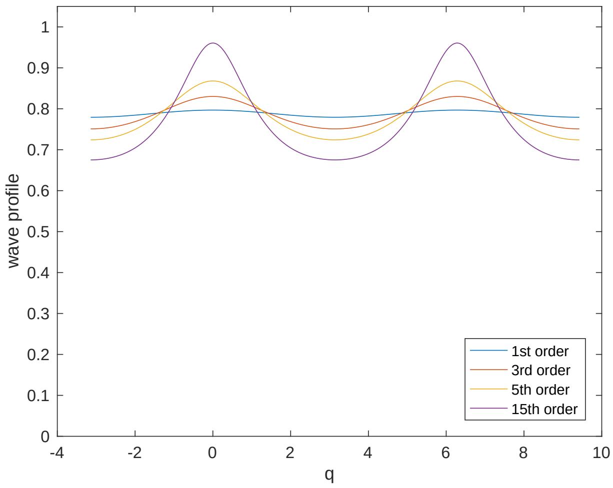

Figure 5: Waveprofiles for waves with residual of same magnitude, $\gamma = 0$.

irrotational case we observe the expected quadratic convergence rate.

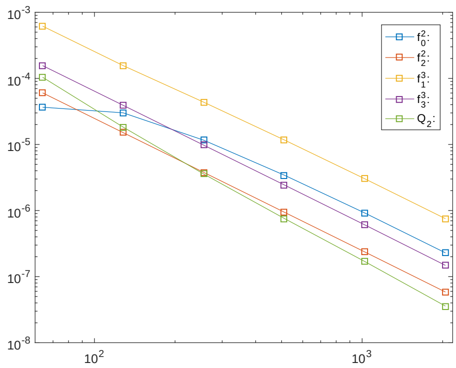

(a) $h_{2,h}, h_{3,h}$ and $Q_{2,h}$

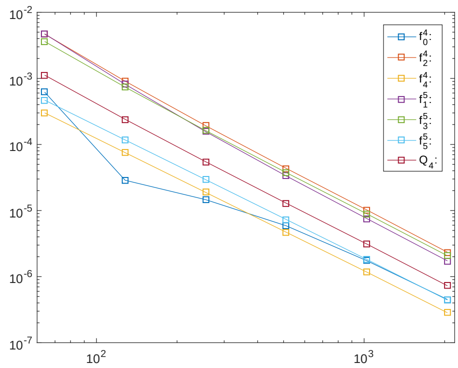

(b) $h_{4,h}, h_{5,h}$ and $Q_{4,h}$

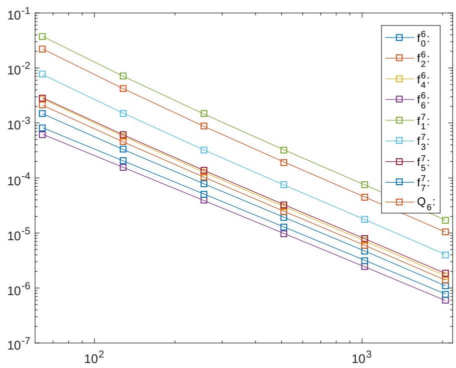

(c) $h_{6,h}, h_{8,h}$ and $Q_{6,h}$

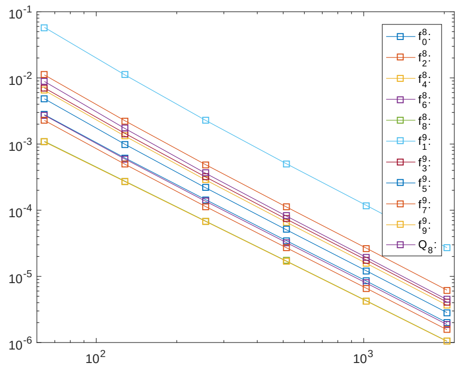

(d) $h_{8,h}, h_{9,h}$ and $Q_{8,h}$

Figure 6: $||f_m^k - f_{m,h}^k||_{L_2}$ and $|Q_k - Q_{k,h}|$ vs. degrees of freedom, $\gamma = 1$.

Table 2 displays residuals of the operators $\mathcal{H}$ and $\mathcal{B}_0$ for the vorticity function $\gamma(-p) = p$. Notable is that the residuals decrease significantly faster that in Table 1. One reason for this is that the considered value $Q = 20.69$ is relatively close to Q^* and thus the values of $b \in [0.0843, 0.0860]$ smaller than in the considered irrotational case. As expected we observe that the error of low order terms, displayed in the third column, is insignificant compared to the residual of high order terms.

	$\lvert\lvert\mathcal{H}[h_h^{(2N+1)}]\rvert\rvert_{L_2}$	$\lvert B_0[h_h^{(2N+1)}, Q_h^{(2N)}]\rvert$	$E_{\mathrm{LO}}(h_h^{(2N+1)})$
$Q_h^{(2)}, h_h^{(3)}$	4.07E-04	5.37E-04	1.59E-09
$Q_h^{(4)}, h_h^{(5)}$	3.49E-05	3.93E-05	1.56E-09
$Q_h^{(6)}, h_h^{(7)}$	2.63E-06	2.90E-06	1.83E-09
$Q_h^{(8)}, h_h^{(9)}$	3.74E-07	3.67E-07	1.19E-09
$Q_h^{(10)}, h_h^{(11)}$	3.19E-08	2.83E-08	1.47E-09
$Q_h^{(12)}, h_h^{(13)}$	2.56E-09	2.56E-09	1.71E-09
$Q_h^{(14)}, h_h^{(15)}$	2.90E-10	2.71E-10	2.29E-09

Table 2: Residual of the differential and boundary operator for $Q = 20.69$ and the relative low order error E_{LO} (25), $\gamma(-p) = p$

Finally we give some examples of the influence of vorticity on wave characteristics. The waves are chosen such that the residual is of same magnitude where the reference was the irrotational wave with $Q = 22.05$. In Figure 4 we observe that negative vorticities allow for larger waves while maintaining the same error.

Acknowledgements

The authors were supported by the project *Computation of large amplitude water waves* (P 27755-N25), funded by the Austrian Science Fund (FWF).

References

[1] A. Constantin, K. Kalimeris, and O. Scherzer. Approximations of steady periodic water waves in flows with constant vorticity. *Nonlinear Analysis: Real World Applications*, 25:276–306, 2015.

[2] A. Constantin and W. Strauss. Exact steady periodic water waves with vorticity. *Communications on Pure and Applied Mathematics*, 57(4):481–527, 2004.

[3] A. D. Craik. The origins of water wave theory. *Annual review of fluid mechanics*, 36, 2004.

[4] K. Kalimeris. Asymptotic expansions for steady periodic water waves in flows with constant vorticity. *Nonlinear Analysis: Real World Applications*, 2017.

[5] P. Karageorgis. Dispersion relation for water waves with non-constant vorticity. *European Journal of Mechanics-B/Fluids*, 34:7–12, 2012.

[6] A. Logg and G. N. Wells. Dolfin: Automated finite element computing. *ACM Transactions on Mathematical Software (TOMS)*, 37(2):20, 2010.

[7] A. Logg, G. N. Wells, and J. Hake. Dolfin: A c++/python finite element library. *Automated Solution of Differential Equations by the Finite Element Method*, pages 173–225, 2012.

[8] J. Nitsche. L-convergence of finite element approximations. *Mathematical aspects of finite element methods*, pages 261–274, 1977.

[9] H. R. Schwarz. *Methode der finiten Elemente: eine Einführung unter besonderer Berücksichtigung der Rechenpraxis*, volume 47. Springer-Verlag, 2013.

[10] G. G. Stokes. On the theory of oscillatory waves. *Trans Cambridge Philos Soc*, 8:441–473, 1847.